Depleting Neuronal PrP in Prion Infection Prevents Disease and Reverses Spongiosis

Giovanna Mallucci *et al.*

Science **302**, 871 (2003);
DOI: 10.1126/science.1090187

nucleosides (*25*). The dxA nucleoside is a violet-blue fluorophore with emission maximum at 389 nm (*26*), and the dxT nucleoside is also violet, with emission at 375 nm. Separate experiments confirmed that both are fluorescent in the context of oligomers. Thus all the base pairs of xDNA are fluorescent, which suggests applications in detection and analysis of natural DNA and RNA.

When all expanded base analogs are placed in one strand, it allows the targeting of natural DNA with enhanced binding affinity. This suggests the use of expanded oligomers (xDNAs) in applications involving hybridization, such as with microarrays, antisense studies, and analytical DNA/RNA detection methods. It remains to be tested whether analogous expanded guanine and cytosine analogs would pair similarly in this context, which would be necessary for generalized targeting of any natural sequence.

We conclude that a genetic base-paired molecular framework is not limited to the size of the DNA helix that evolved in terrestrial biology. It is noteworthy that one significant difference of this expanded-size genetic system, relative to the natural one, is its increased potential for encoding information (*27*). Pairing of four expanded bases with the four natural bases in all complementary combinations would be expected to yield eight base pairs of information encoding ability.

References and Notes

1. A. Murakami, K. R. Blake, P. S. Miller, *Biochemistry* **24**, 4041 (1985).
2. M. Matsukura *et al.*, *Proc. Natl. Acad. Sci. U.S.A.* **84** 7706 (1987).
3. M. Egholm *et al.*, *Nature* **365**, 566 (1993).
4. A. Eschenmoser, *Science* **284**, 2118 (1999).
5. A. A. Koshkin *et al.*, *Tetrahedron* **54**, 3607 (1998).
6. H. P. Rappaport, *Nucleic Acids Res.* **16**, 7253 (1988).
7. S. A. Benner *et al.*, *Pure Appl. Chem.* **70**, 263 (1998).
8. T. J. Matray, E. T. Kool, *J. Am. Chem. Soc.* **120**, 6191 (1998).
9. D. L. McMinn *et al.*, *J. Am. Chem. Soc.* **121**, 11585 (1999).
10. T. Mitsui *et al.*, *J. Am. Chem. Soc.* **125**, 5298 (2003).
11. K. Tanaka, A. Tengeiji, T. Kato, N. Toyama, M. Shionoya, *Science* **299**, 1212 (2003).
12. R. A. Lessor, K. J. Gibson, N. J. Leonard, *Biochemistry* **23**, 3868 (1984).
13. N. J. Leonard, M. A. Sprecker, A. G. Morrice, *J. Am. Chem. Soc.* **98**, 3987 (1976).
14. J. Michel, J. J. Toulme, J. Vercauteren, S. Moreau, *Nucleic Acids Res.* **24**, 1127 (1996).
15. M. Hoffer, *Chem. Ber.* **93**, 2777 (1960).
16. Details of nucleoside phosphoramidite synthesis and characterization, of oligonucleotide synthesis, and of thermodynamics methods are given in the Supporting Online Material.
17. H. Liu, J. Gao, E. T. Kool, unpublished observations.
18. Hyperchromicity values of helices involving the expanded bases should not be directly compared with those of natural DNAs because the photophysical properties of xT and xA are different from those of T and A.
19. G. Prakash, E. T. Kool, *J. Am. Chem. Soc.* **114**, 3523 (1992).
20. Thermal denaturation of the two single-stranded components alone under these conditions (5.0 μM in oligonucleotide) revealed transition temperatures of 26.5 and 27.5°C, significantly lower than that of the duplex.
21. F. Seela, A. Melenewski, C. Wei, *Bioorg. Med. Chem. Lett.* **17**, 2173 (1997).
22. K. Groebke *et al.*, *Helv. Chim. Acta* **81**, 375 (1998).
23. M. F. H. Hoffmann, A. M. Brückner, T. Hupp, B. Engels, U. Diederichsen, *Helv. Chim. Acta* **83**, 2580 (2000).
24. F. Seela, C. Wei, A. Melenewski, E. Feiling, *Nucleosides Nucleotides* **17**, 2045 (1998).
25. H. Liu, J. Gao, L. Maynard, D. Saito, E. T. Kool, in preparation.
26. R. F. Kauffman, H. A. Lardy, J. R. Barrio, M. C. G. Barrio, N. J. Leonard, *Biochemistry* **17**, 3686 (1978).
27. J. A. Piccirilli, T. Krauch, S. E. Moroney, S. A. Benner, *Nature* **343**, 33 (1990).

28. We thank N. J. Leonard for helpful discussions. This work was supported by NIH grants GM63587 and GM52956. H. L. and J. G. acknowledge support from Stanford Graduate Fellowships.

Supporting Online Material

www.sciencemag.org/cgi/content/full/302/5646/868/DC1
Materials and Methods
Figs. S1 and S2
Tables S1 and S2
References and Notes

23 June 2003; accepted 12 September 2003

Depleting Neuronal PrP in Prion Infection Prevents Disease and Reverses Spongiosis

Giovanna Mallucci, Andrew Dickinson, Jacqueline Linehan, Peter-Christian Klöhn, Sebastian Brandner, John Collinge*

The mechanisms involved in prion neurotoxicity are unclear, and therapies preventing accumulation of PrP^{Sc}, the disease-associated form of prion protein (PrP), do not significantly prolong survival in mice with central nervous system prion infection. We found that depleting endogenous neuronal PrP^{c} in mice with established neuroinvasive prion infection reversed early spongiform change and prevented neuronal loss and progression to clinical disease. This occurred despite the accumulation of extraneuronal PrP^{Sc} to levels seen in terminally ill wild-type animals. Thus, the propagation of non-neuronal PrP^{Sc} is not pathogenic, but arresting the continued conversion of PrP^{c} to PrP^{Sc} within neurons during scrapie infection prevents prion neurotoxicity.

Prion diseases are fatal transmissible neurodegenerative diseases, characterized pathologically by widespread neuronal loss, spongiform change, and the accumulation of PrP^{Sc}, the pathological isoform of a host-encoded prion protein (PrP^{c}). However, the cause of neuronal death in prion disease remains unclear. Thus, although PrP^{Sc} is associated with both infectivity and pathological changes, levels of PrP^{Sc} in the brain may not correlate with symptoms in prion-infected mice (*1*–*4*), and there are human prion diseases with little or no detectable PrP^{Sc} (*5*, *6*). Further, PrP^{Sc} itself is not toxic to brain tissue that does not express PrP^{c} and cannot replicate prions (*1*, *2*, *7*). Also, compounds that reduce PrP^{Sc} accumulation in prion-infected cells in culture have only modest effects in vivo on disease incubation periods in prion-infected mice and only when coadministered with the prion inoculum or very soon after infection (*8*, *9*). No treatment has been effective in animals after the onset of clinical signs of disease, and no agent has prevented disease progression in mice during the asymptomatic preclinical phase of central nervous system (CNS) scrapie infection, when intervention would have the greatest therapeutic potential (*10*, *11*). The conversion of PrP^{c} to PrP^{Sc} is intrinsic to the pathological process, however, because mice devoid of PrP^{c} ($Prnp^{0/0}$) are resistant to prion disease and do not propagate infectivity (*1*, *2*, *12*). Similarly, PrP-null brain tissue surrounding prion-infected $Prnp^{+/+}$ neurografts does not develop prion neuropathological change (*7*). Targeting PrP^{c} itself, as opposed to PrP^{Sc}, in established prion infection directly removes the substrate for further conversion and prion replication and might be expected to be a more effective therapeutic strategy than reduction of PrP^{Sc} accumulation.

We tested the effects of neuronal PrP^{c} depletion in animals with established neuroinvasive scrapie on the subsequent course of disease and neuropathological changes. We have previously shown that acquired neuronal PrP^{c} depletion in adult mice is in itself without major detrimental effects (*13*). In another mouse model of acquired PrP knock-out, only the effects of PrP^{c} depletion before inoculation with scrapie prions were studied (*14*), essentially replicating the inoculation of $Prnp^{0/0}$ animals; the effects of PrP^{c} depletion after scrapie infection were not examined. We used two lines of transgenic M*lox*P mice, tg37 and tg46, that express PrP^{c} from M*lox*P transgenes at ~3 and 1 times wild-type levels, respectively, and that normally succumb to scrapie ~12 and 18 weeks, respectively, after intracerebral Rocky Mountain Laboratory (RML) scrapie prion inoculation (Figs. 1 and 2). PrP^{c} expression in these mice (which were generated on a $Prnp^{0/0}$ background) can be eliminated by the action of

Medical Research Council Prion Unit and Department of Neurodegenerative Disease, Institute of Neurology, Queen Square, London WC1, UK.

*To whom correspondence should be addressed. E-mail: j.collinge@prion.ucl.ac.uk

the enzyme Cre recombinase (*15*), which excises the (floxed) PrP-coding sequences in the M*lox*P transgenes. NFH-Cre mice express Cre under the control of the neurofilament heavy chain (NFH) promoter (*16*) at ~10 to 12 weeks of age, which results in Cre-mediated recombination of floxed transgenes in neuronal cells but not in astrocytes or other cell types (fig. S1). Thus, double transgenic NFH-Cre/M*lox*P mice express PrP in neurons and nonneuronal cells until ~12 weeks of age, when they undergo Cre-mediated depletion of neuronal PrP^c (*13*).

We inoculated NFH-Cre/M*lox*P mice with RML scrapie prions at 3 to 4 weeks of age on weaning, allowing prion replication and CNS infection to proceed normally until Cre-mediated neuronal PrP^c depletion occurred. M*lox*P mice without the NFH-Cre transgene were inoculated in parallel. Animals were examined daily and were culled for analysis of neuropathological changes at two-week intervals after inoculation (*17*). We confirmed M*lox*P transgene recombination in the brains of double transgenic animals by Southern analysis of whole-brain DNA at around 8 weeks postinoculation (wpi) (fig. S2), at which stage they were 11 to 12 weeks old, consistent with our previous findings (*13*). Correspondingly, total brain PrP expression, determined by semiquantitative immunoblotting (*17*), was similar in all mice before 8 wpi, at which point it declined in animals with Cre-mediated recombination (fig. S3).

At this time point, all animals with and without Cre expression showed pathological evidence of neuroinvasive CNS scrapie infection to a similar extent. Specifically, there was PrP^{Sc} deposition and reactive astrocytosis in thalamus, hippocampus, and cortex (Fig. 3, E, G, Q, and U). In scrapie-infected NFH-Cre/tg37 and tg37 mice (but not in tg46 mice), there was also early spongiform degeneration, notably in the hippocampus (Figs. 1 and 3, A, C, I, and M). The early appearance of spongiosis in these animals may reflect the higher level of expression of PrP^c and short scrapie incubation period of tg37 mice compared with tg46 mice. Similar levels of PrP^{Sc} were also found in all mice at 8 wpi with the use of semiquantitative immunoblotting, but were just within the limits of detection with the use of conventional methods, and were confirmed by sodium phosphotungstic acid precipitation of PrP^{Sc} from brain homogenates (*17*, *18*) (fig. S4).

The depletion of neuronal PrP^c in animals with established CNS scrapie prevented progression to clinical prion disease and resulted in the long-term survival of infected animals. To date, prion-infected NFH-Cre/tg37 and NFH-Cre/tg46 mice remain asymptomatic at >57 wpi ($n = 6$) and >58 wpi ($n = 3$), respectively, whereas tg37 and tg46 mice infected at the same time died after 12 weeks (84 ± 5 days, $n = 6$) and 18 weeks (120 ± 2 days, $n = 8$), respectively (Figs. 1 and 2). This represents a >fourfold increase in scrapie incubation time for NFH-Cre/tg37 animals (~threefold for NFH-Cre/tg46 mice), approaching the normal life-span of a mouse.

Neuropathologically, asymptomatic prion-infected animals with PrP^c depletion were protected from neuronal loss up to 48 wpi. In scrapie-infected tg37 mice without PrP depletion, hippocampal CA1 to CA3 neurons began to degenerate from 10 wpi, with almost complete CA1 to CA3 cell loss by 12 wpi and accompanying shrinkage of the entire hippocampus (Fig. 3, B and D). Similar changes were seen in terminally ill tg46 mice by 18 wpi, establishing a correlation between development of clinical symptoms in RML scrapie infection and neuronal loss in M*lox*P mice. In contrast, in scrapie-infected NFH-Cre/M*lox*P mice, CA1 to CA3 neurons remained healthy, and hippocampal structure was completely preserved (Fig. 3, I to L and M to P), demonstrating the neuroprotection afforded by depleting neuronal PrP^c in established CNS scrapie infection.

Further, the hippocampus was also free of spongiosis (intraneuronal vacuoles in cells that have not yet degenerated) in scrapie-infected mice after neuronal PrP^c depletion. We found early spongiform change in both tg37 and NFH-Cre/tg37 mice at 8 wpi (Figs. 1 and 3, C and M) but not in age-matched uninfected controls (fig. S5) nor in mice with Cre-mediated neuronal PrP^c depletion examined as early as 10 wpi, up to 48 wpi (Figs. 1 and 3, N, O, and P, and fig. S5). Thus it appears that there was reversal of early

		wpi													
		2	8	10	12	14	16	18	20	22	26	33	48	49	52
tg37	Symptoms	-	-	+	+++	DEATH									
	Neuronal loss	-	-	++	+++										
	PrP^{Sc}	-	+	+++	+++										
	Gliosis	-	+	+++	+++										
	HC spongiosis	-	+	+++	+++										
NFH-Cre/tg37	Symptoms	-	-	-	-	-	-	-	-	-	-	-	-	-	-
	Neuronal loss	-	-	-	-	-	-	-			-	-	-		
	PrP^{Sc}	-	+	+	+	+	+	+			++	+++	+++		
	Gliosis	-	+	+	+	+	+	+			++	+++	+++		
	HC spongiosis	-	+	-	-	-	-	-			-	-	-		
tg46	Symptoms	-	-	-	-	-	+	+++	DEATH						
	Neuronal loss	-	-	-	-	-	++	+++							
	PrP^{Sc}	-	+	+	++	++	++	+++							
	Gliosis	-	+	+	++	++	++	+++							
	HC spongiosis	-	-	-	++	++	+++	+++							
NFH-Cre/tg46	Symptoms	-	-	-	-	-	-	-	-	-	-	-	-	-	-
	Neuronal loss	-	-	-	-	-	-	-	-	-	-			-	
	PrP^{Sc}	-	+	+	+	+	+	++	++	++	++			+++	
	Gliosis	-	+	+	+	+	+	++	++	++	++			+++	
	HC spongiosis	-	-	-	-	-	-	-	-	-	-			-	

Fig. 1. Clinical and neuropathological features of scrapie-infected mice with and without neuronal PrP^c depletion. HC, hippocampus; –, absent; +, ++, +++ indicate mild, moderate, and severe, respectively; + symptoms represented disheveled appearance and poor grooming. At all time points, $n = 3$ to 6 animals, except at 48 and 49 wpi, when $n = 2$. Arrow indicates onset of Cre-mediated PrP^c depletion.

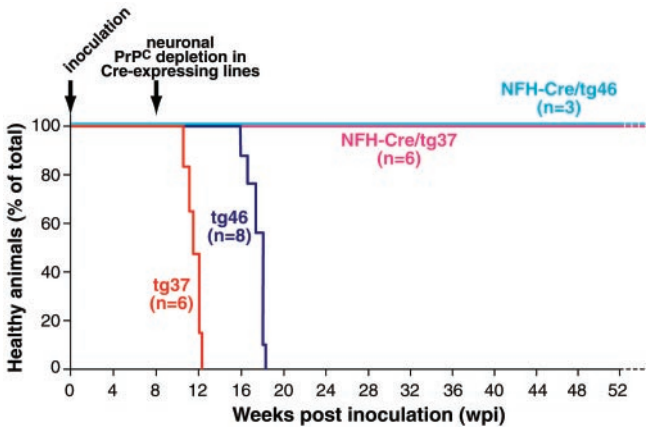

Fig. 2. Survival of scrapie-infected NFH-Cre/M*lox*P mice after Cre-mediated PrP^c depletion. All tg37 and tg46 mice succumbed to scrapie within 12 and 18 wpi, respectively. No animals with Cre-mediated PrP^c depletion at 8 wpi have succumbed to scrapie or show any clinical signs of disease by 52 wpi. Onset of Cre-mediated PrP^c depletion in NFH-Cre/M*lox*P mice, 8 weeks into the course of infection, is indicated.

spongiosis in double transgenic animals after PrP^c depletion. Because spongiform pathology at 8 wpi was relatively subtle, coinciding with the onset of Cre-mediated PrP depletion, we further inoculated animals at 1 week of age (*19*) to allow more time for development of prion pathology before PrP^c depletion. Under these conditions, there was unequivocal spongiform change at 8 wpi (Fig. 3, C and M), which similarly reversed when Cre was expressed at the relatively later time point of 10 wpi in these animals, when they were aged ~11 weeks (fig. S5). Although in this model early spongiosis was not associated with the diagnostic neurological signs of murine scrapie, in humans this stage of prion infection may correspond to the early clinical stages of disease, which may be relatively prolonged and where any potential for reversal of pathology would be most important.

The pattern of neuroprotection observed in scrapie-infected NFH-Cre/M*lox*P mice correlated well with the known pattern of Cre expression in NFH-Cre mice (*13*), being strongest in neuron-rich regions, in particular in the entire hippocampus. A degree of spongiform change was seen in these mice in other brain regions at late time points, notably in some cortical regions, deep white matter tracts, and cerebellum, and may reflect lower density neuronal populations and hence less overall NFH-Cre transgene expression in these regions. Importantly, however, these mice remained asymptomatic (Fig. 1).

However, we did observe increasing gliosis and PrP^{Sc} deposition in infected animals after PrP^c depletion. Most notably, PrP^{Sc} accumulation progressed over prolonged periods of observation (Fig. 3, Q to T) and was clearly detected by immunoblotting in NFH-Cre/tg37 mice at 12 wpi, and in NFH-Cre/tg46 mice by 18 wpi (Fig. 4), but was not associated with neuronal loss or clinical symptoms. In NFH-Cre/tg46 mice, levels of PrP^{Sc} increased significantly by 49 wpi (Fig. 4A), and, in NFH-Cre/tg37 mice, PrP^{Sc} levels at 48 wpi were equivalent to those seen in terminally ill tg37 mice at 12 wpi and in end-stage RML-scrapie–inoculated wild-type mice (Fig. 4B).

The continued accumulation of PrP^{Sc} in this model after neuronal PrP^c depletion is likely to reflect prion replication predominantly in glial cells where Cre was not expressed (fig. S1) and PrP^c not depleted: Both microglia (*20*) and astrocytes (*21*) support scrapie replication. Because astrocytes are the largest nonneuronal PrP^c-expressing population of cells in the brain, they are probably the major source of continued PrP^{Sc} generation here. Prominent astrocytosis is a feature even of uninfected FVB mice (*22*) (fig. S5) [the predominant genetic background of these transgenic lines (*13*)], but here we found continued astrocytic proliferation in all animals with a notable increase over time (Fig. 3, U to X), in parallel to and correlating with the pattern of continued PrP^{Sc} deposition (Fig. 3, Q to T). We found that PrP^{Sc} deposits colocalized with astrocytes in the brains of infected mice with neuronal PrP^c depletion with the use of dual immunofluorescent labeling for PrP and for the astrocytic marker glial fibrillary acidic protein (GFAP) (*17*), which was not seen in scrapie-infected control animals without PrP depletion (fig. S6). The fact that these mice remain asymptomatic indicates that even extensive extraneuronal PrP^{Sc} replication does not cause clinical disease or neurodegeneration in this model (*23*). In contrast, the dramatic neuronal loss and clinical signs seen in M*lox*P mice, where PrP^c was not depleted in neurons, suggest that it is the conversion of PrP^c to disease-associated isoforms specifically within neurons that is neurotoxic.

Also, we found that after PrP^c depletion the infectivity in brain homogenates from scrapie-infected NFH-Cre/M*lox*P lagged behind that of animals without the Cre transgene by 1 to 2 log infectious units but eventually reached maximally infectious titers by 48 wpi (table S1 and fig. S7). This initial lag is consistent with loss of neuronal propagation of infectivity, with subsequent predominantly astrocytic propagation of infectivity, as occurs in GFAP-PrP mice (*21*). In-

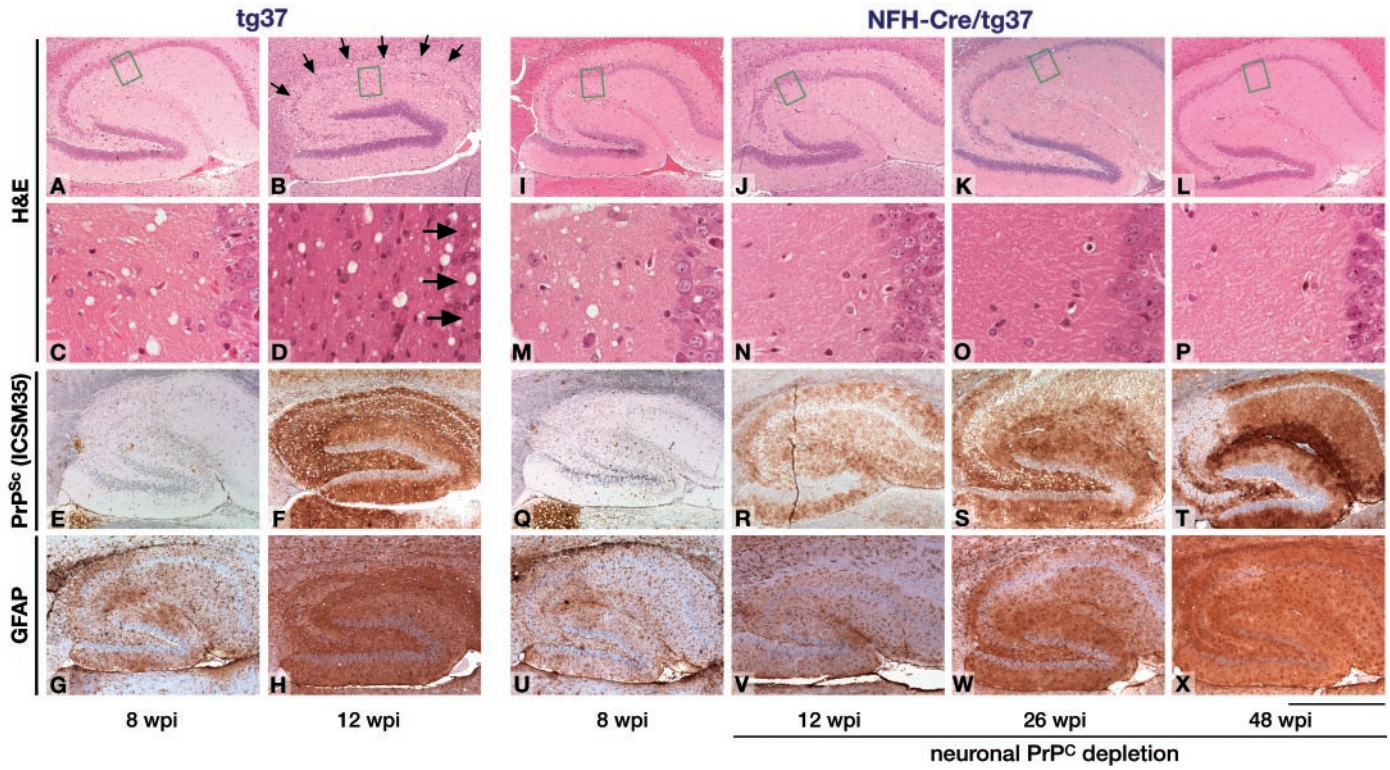

Fig. 3. Prevention of neuronal loss and reversal of early spongiosis in scrapie-infected mice after PrP^c depletion. Fixed sections show hippocampal region from scrapie-infected tg37 and NFH-Cre/tg37 mice at various time points postinfection. Sections were stained with haematoxylin and eosin (H&E) and immunostained for detection of astrocytosis and PrP^{Sc} deposition. There is severe loss of CA1 to CA3 neurons (arrows) (**B** and **D**) with shrinkage of the entire hippocampus (B) in terminally ill tg37 mice but no neuronal loss in asymptomatic prion-infected mice with Cre-mediated PrP^c depletion [(**J**), (**K**), and (**L**)] up to 48 wpi. Early spongiosis was seen in eight out of eight animals at 8 wpi (**C** and **M**), but was not seen at 12, 26, and 48 wpi in NFH-Cre/tg37 mice [(**N**), (**O**), and (**P**)], despite continued PrP^{Sc} accumulation and gliosis [(**R**) to (**T**) and (**V**) to (**X**)]. Scale bar represents 320 μm, except in panels (C), (D), and (M) to (P), where it represents 80 μm.

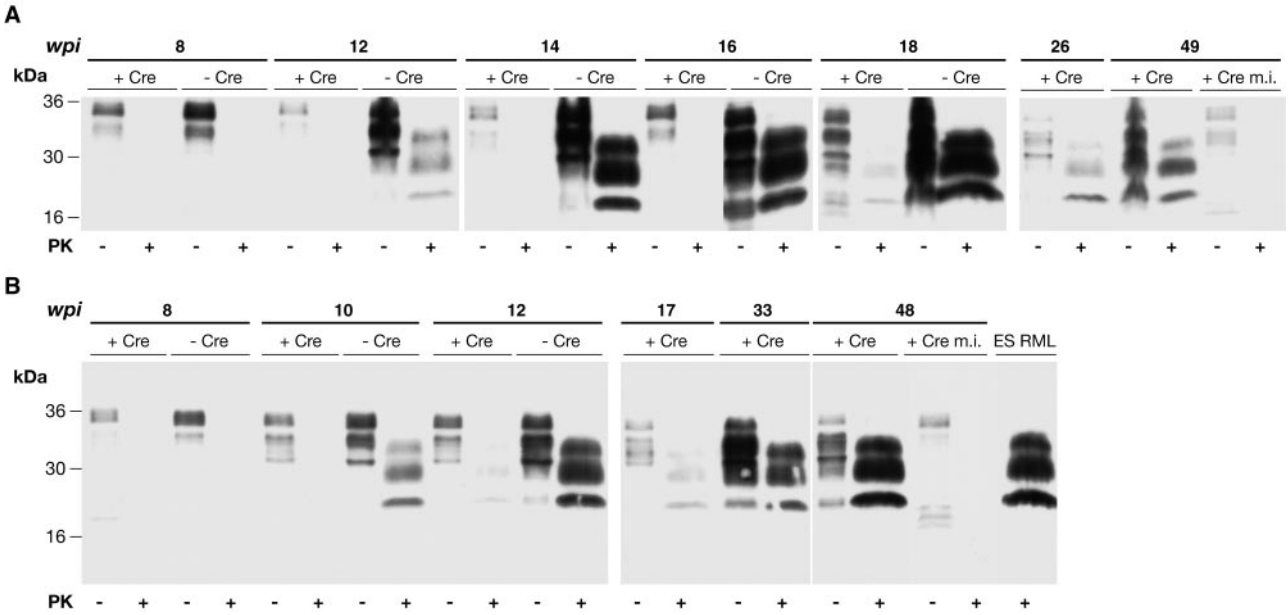

Fig. 4. Immunoblot analysis of total PrP in scrapie-infected mice with and without PrP^c depletion. SDS–polyacrylamide gel electrophoresis of 10% whole-brain homogenates pre– (–) and post– (+) proteinase K (PK) digestion from scrapie-infected tg46 and NFH-Cre/tg46 mice (**A**) and tg37 and NFH-Cre/tg37 mice (**B**) from each time point. 10 μl was loaded per lane. Total PrP was detected with the use of ICSM35 antibody (*25*). "+Cre" and "–Cre" denote the presence or absence of Cre-mediated PrP^c depletion, respectively. PrP^{Sc} continues to accumulate in M*lox*P mice after PrP^c depletion and is first easily detected at 18 and 12 wpi in NFH-Cre/tg46 and NFH-Cre/tg37 brains, respectively. Samples from a terminally ill RML-inoculated wild-type mouse (ES RML) and from mock-inoculated (m.i.) NFH-Cre/M*lox*P mice were included as controls. kDa, kilodaltons.

deed, high levels of prion infectivity are also found in microglia extracted from scrapie-infected mouse brains despite low levels of total PrP (*24*).

It is possible that the rate of PrP^{Sc} accumulation is also an important factor in development of symptomatic prion disease. In scrapie-infected wild-type and hemizygous $Prnp^{0/+}$ mice, levels of total PrP (PrP^c and PrP^{Sc}) increase markedly during the course of disease, compared to basal levels of PrP expression (*1*). We found a similar increase in scrapie-infected tg46 mice between 8 wpi and 18 wpi (–Cre, Fig. 3A) and tg37 mice between 8 wpi and 12 wpi (–Cre, Fig. 3B), where the rise to end-stage levels of PrP^{Sc} occurs in ~2 weeks, at which stage the mice become clinically affected and die. Total PrP levels also increase in prion-infected mice with neuronal PrP^c depletion, presumably reflecting continued glial PrP^{Sc} replication (Fig. 3, A and B, +Cre), but the increase to end-stage levels of PrP^{Sc} in NFH-Cre/tg37 takes ~36 weeks and produces no symptoms.

In conclusion, we have demonstrated an intervention that prevents the development of symptomatic prion disease in mice with established CNS scrapie infection. Our strategy of arresting neuronal conversion of PrP^c to PrP^{Sc} by depleting the former prevents progression from preclinical CNS prion infection to clinically manifest disease. PrP-null mice and $Prnp^{0/0}$ brain tissue surrounding prion-infected $Prnp^{+/+}$ neurografts are resistant to prion disease (*1*, *2*, *7*), because these tissues do not express PrP^c and cannot propagate prions. In contrast, we have shown reversal of early neurodegenerative changes of CNS prion infection and long-term protection against neuronal loss despite continued prion replication and PrP^{Sc} depostion. Our results also argue against direct neurotoxicity of PrP^{Sc}, because the continued nonneuronal replication and accumulation of PrP^{Sc} throughout the brains of scrapie-infected mice is not pathogenic. Indeed, this may explain the lack of significant efficacy in vivo of therapeutic agents that reduce PrP^{Sc} accumulation in vitro. It appears that the conversion of PrP^c to disease-related forms must occur within neurons to be pathogenic, consistent with the possibility that a toxic intermediate is generated within neurons during the conversion process (*4*). These findings provide a rationale for targeting PrP^c as a therapeutic intervention in prion disease, which could prevent the progression to clinical disease in presymptomatic individuals infected with prions or with pathogenic *PRNP* mutations.

References and Notes

1. H. Bueler *et al*., *Cell* **73**, 1339 (1993).
2. J. C. Manson, A. R. Clarke, P. A. McBride, I. McConnell, J. Hope, *Neurodegeneration* **3**, 331 (1994).
3. M. Fischer *et al*., *EMBO J.* **15**, 1255 (1996).
4. A. F. Hill *et al*., *Proc. Natl. Acad. Sci. U.S.A.* **97**, 10248 (2000).
5. R. Medori *et al*., in *Prion Diseases of Humans and Animals*, S. B. Prusiner, J. Collinge, J. Powell, B. Anderton, Eds. (Ellis Horwood, London, 1992), chap. 18.
6. J. Collinge *et al*., *Lancet* **346**, 569 (1995).
7. S. Brandner *et al*., *Nature* **379**, 339 (1996).
8. A. Aguzzi, M. Glatzel, F. Montrasio, M. Prinz, F. L. Heppner, *Nature Rev. Neurosci.* **2**, 745 (2001).
9. F. Tagliavini *et al*., *Science* **276**, 1119 (1997).
10. S. J. Collins *et al*., *Ann. Neurol.* **52**, 503 (2002).
11. S. A. Priola, A. Raines, W. S. Caughey, *Science* **287**, 1503 (2000).
12. A. Sailer, H. Bueler, M. Fischer, A. Aguzzi, C. Weissmann, *Cell* **77**, 967 (1994).
13. G. R. Mallucci *et al*., *EMBO J.* **21**, 202 (2002).
14. P. Tremblay *et al*., *Proc. Natl. Acad. Sci. U.S.A.* **95**, 12580 (1998).
15. B. Sauer, N. Henderson, *Proc. Natl. Acad. Sci. U.S.A.* **85**, 5166 (1988).
16. J. P. Julien *et al*., *Gene* **68**, 307 (1988).
17. Materials and methods are available as supporting material on *Science* Online.
18. J. Safar *et al*., *Nature Med.* **4**, 1157 (1998).
19. This step was done after further appropriate Home Office License approval was obtained.
20. C. A. Baker, Z. Y. Lu, I. Zaitsev, L. Manuelidis, *J. Virol.* **73**, 5089 (1999).
21. A. J. Raeber *et al*., *EMBO J.* **16**, 6057 (1997).
22. M. F. Goelz *et al*., *Lab. Anim. Sci.* **48**, 34 (1998).
23. In apparent conflict with our data, GFAP-PrP mice expressing hamster PrP^c in astrocytes succumbed to infection with hamster scrapie strain 263K (*21*). However, the two models are not directly comparable, because they were generated on different genetic backgrounds and differ with respect to the species of PrP expressed, the promoters used, and the scrapie strains used for infection. GFAP-PrP mice overexpress hamster PrP^c in astrocytes because of exponential induction of the GFAP promoter during infection, whereas in M*lox*P mice there is low-level astrocytic expression of mouse PrP^c expression under its own promoter. Further, 263K scrapie used to infect the GFAP-PrP mice produces very little neuronal loss, in contrast to the severe neurodegeneration induced by RML infection of M*loxP* mice.
24. C. A. Baker, D. Martin, L. Manuelidis, *J. Virol.* **76**, 10905 (2002).
25. E. A. Asante *et al*., *EMBO J.* **21**, 6358 (2002).

26. We thank P. Hudson, C. O'Malley, J. Beake, D. Moore, H. Westby, and R. Ahmet for technical assistance and R. Young for help with graphics. This work was funded by the Medical Research Council, UK.

Supporting Online Material

www.sciencemag.org/cgi/content/full/302/5646/871/DC1
Materials and Methods
Figs. S1 to S7
Table S1

7 August 2003; accepted 29 September 2003